NASA TN D-292

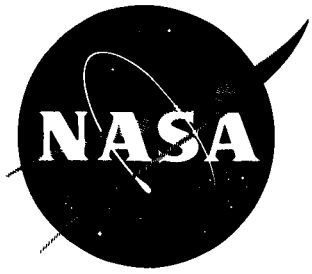

TECHNICAL NOTE

D-292

AN INTEGRAL METHOD FOR NATURAL-CONVECTION FLOWS AT HIGH AND LOW PRANDTL NUMBERS

By Willis H. Braun and John E. Heighway

Lewis Research Center
Cleveland, Ohio

NATIONAL AERONAUTICS AND SPACE ADMINISTRATION

WASHINGTON June 1960

NATIONAL AERONAUTICS AND SPACE ADMINISTRATION

TECHNICAL NOTE D-292

AN INTEGRAL METHOD FOR NATURAL-CONVECTION FLOWS AT HIGH AND LOW PRANDTL NUMBERS

By Willis H. Braun and John E. Heighway

SUMMARY

The boundary layer is analyzed into two regions, the thermal and the viscous. Separate polynomials are used to approximate the temperature and velocity profiles in the two regions and are then matched at the interface. Comparisons with numerical solutions of the flow over a flat plate show improvements over other integral methods. Application is made to the flow over a cone.

INTRODUCTION

The nonlinear character of the boundary-layer equations has made necessary in the past the development of approximate, integral methods for their solution. While eliminating much cumbersome numerical calculation, these methods also obtain with reasonable accuracy some of the gross characteristics of the boundary layer. In forced-convection boundary-layer flow the Kármán-Pohlhausen method has long been the model for this type of solution. Even with the advent of fast digital computers, integral methods have their place as a source of rapid, approximate answers without the computation of large numbers of velocity and temperature profiles.

The integral method most often employed in natural-convection boundary-layer flows is attributed to Squire and is described in the volumes by Eckert (ref. 1) and Goldstein (ref. 2). Levy (ref. 3) has illustrated its application to several kinds of bodies. This integral method predicts heat transfer with acceptable accuracy, around 13 percent at low Prandtl number and 3 percent at high Prandtl number. However, the error in skin friction can be very large, as much as 100 percent, and the mass flow may be in error by an order of magnitude. These discrepancies are results of the choice of temperature and velocity profiles, especially the restriction that they extend the same distance from the wall, that is, that the viscous and thermal boundary layers are equal. A very viscous fluid (high Prandtl number) is known to have a much larger

viscous than thermal boundary layer (Ostrach, ref. 4), whereas a highly heat-conducting fluid (low Prandtl number) has a viscous layer much smaller than the thermal layer. Formerly the errors in mass flow were of no consequence, for they were entirely separate from the heat-transfer results; but now, when problems involving velocity-dependent forces can be anticipated, it is necessary to have better approximations to the velocity profiles. Such will be the case, for example, in rotating systems (Coriolis force) and electrically conducting fluids (magnetohydrodynamic forces).

It becomes evident, then, that if the integral method is to perform satisfactorily, especially at extremes of Prandtl number, the velocity and temperature profiles must be made more flexible. Preferably, their forms should change regularly with Prandtl number between their limiting forms at zero and infinite Prandtl number. Some progress in this direction has been made in the recent papers of Yamagata (ref. 5) and Fujii (ref. 6), in which they propose velocity profiles having a free parameter determined by the Prandtl number. Fujii's profile includes the feature of variable thickness; but, although it leads to good heat-transfer values over a wide range of Prandtl number, the mass flow vanishes at very large and very small Prandtl numbers.

In this report an integral method that provides flexible profiles over most of the range of Prandtl number is developed. In the beginning, the method is limited to the flow about a flat plate at constant temperature. After the new method is tested against known numerical solutions, it is extended to other bodies on which the flows have the property of similarity. An examination of the differential equations of motion indicates that it is necessary to construct two sets of profiles, one at low Prandtl number and one at high Prandtl number. Separate, parallel developments are made for ease of reference by the reader. This analysis of the differential equations leads to the limiting forms found by LeFevre (ref. 7); however, the present discussion is given in more detail.

FLAT-PLATE FLOW AT LOW PRANDTL NUMBER

Differential Equations at Low Prandtl Number

Consider the steady boundary-layer flow along a vertical plate heated to a uniform temperature T_w. (All symbols are defined in appendix A.) At values of the Prandtl number considerably below unity, the conditions are qualitatively as shown in sketch (a). At a distance up the plate $X = L$, the temperature of the wall influences the temperature of the fluid to a distance Δ_T; that is, Δ_T is the distance at which the difference of the temperature from the ambient T_∞ has

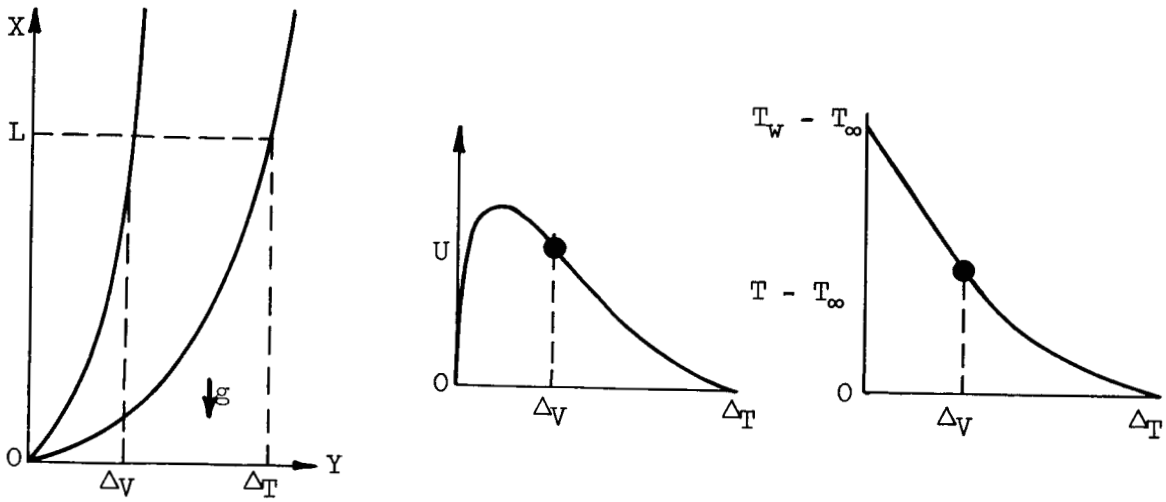

(a)

dropped by an order of magnitude. The kinematic viscosity is small compared with the thermal diffusivity, so that the distance Δ_V from wall to which the viscous forces influence the flow is small compared with Δ_T. The velocity and temperature profiles display qualities characteristic of the two regions. The velocity profile in the thermal region ($\Delta_V < Y \leq \Delta_T$) is that of an inviscid fluid driven by the buoyancy force. In the viscous region ($0 < Y < \Delta_V$), the curvature is reversed, and the profile obeys the no-slip condition at the wall. The temperature profile in the thermal region is the result of a balance of conduction and convection of heat; in the viscous region the main effect is conduction, and consequently the profile is nearly linear.

Thermal region. - The dimensional equations that govern the flow for small temperature differences and no dissipation are (ref. 2):

Continuity:

$$U_X + V_Y = 0 \tag{1a}$$

Momentum:

$$UU_X + VU_Y = \nu U_{YY} + g\beta(T - T_\infty) \tag{1b}$$

Energy:

$$UT_X + VT_Y = \alpha T_{YY} \tag{1c}$$

It is desired to nondimensionalize both dependent and independent variables in a manner that will leave the dependent variables and their

derivatives at unit order of magnitude in the thermal region. At the longitudinal position $X = L$, let representative velocities be $U = U^*$ and $V = V^*$ (as yet undetermined). A set of dimensionless variables x, y, u, v, t is then defined by

$$X = Lx, \quad Y = \Delta_T y, \quad U = U^* u, \quad V = V^* v, \quad T - T_\infty = (T_w - T_\infty)t \tag{2}$$

Under this transformation equations (1) become

$$u_x + \frac{V^* L}{U^* \Delta_T} v_y = 0 \tag{3a}$$

$$uu_x + \frac{V^* L}{U^* \Delta_T} vu_y = \frac{\nu L}{U^* \Delta_T^2} u_{yy} + \frac{g\beta(T_w - T_\infty)L}{(U^*)^2} t \tag{3b}$$

$$ut_x + \frac{V^* L}{U^* \Delta_T} vt_y = \frac{\alpha L}{U^* \Delta_T^2} t_{yy} \tag{3c}$$

The manner in which the magnitudes have been extracted from the dimensional variables in (2) assures that each of the derivatives in (3) is of unit order of magnitude, at least around $X = L$.

In order that both terms of the continuity equation (3a) be of the same order of magnitude, it follows that

$$V^* = \frac{\Delta_T}{L} U^* \tag{4}$$

(where an arbitrary constant of proportionality has been set equal to 1). In the energy equation (3c), the convective heat transfer and the conduction term must balance; this suggests setting

$$\Delta_T = \sqrt{\frac{\alpha L}{U^*}} \tag{5}$$

to keep both sets of terms at the same order of magnitude.

The momentum equation (3b) describes the balance of forces in the fluid. In the thermal region, as mentioned before, the viscous forces are not expected to have much effect. Thus the buoyancy force, which drives the motion, is just balanced by the inertia force, that is, by the rate at which the fluid is gaining momentum. If equations (4) and (5) are used in the momentum equation (3b) with the further requirement that in the thermal region the inertia terms and the buoyancy force must be comparable in magnitude, the characteristic velocity is found to be

$$U^* = \sqrt{g\beta(T_w - T_\infty)L} \tag{6}$$

The velocity U^*, although not given explicitly in the literature, is also the effective result of other nondimensionalizations (e.g., ref. 4).

The set of governing equations for the thermal layer has now been reduced to the form

$$u_x + v_y = 0 \tag{7a}$$

$$uu_x + vu_y = Pr\, u_{yy} + t \tag{7b}$$

$$ut_x + vt_y = t_{yy} \tag{7c}$$

where

$$\left.\begin{aligned} x &= X/L, \quad y = (Gr\ Pr^2)^{1/4} \\ u &= (Gr\ Pr^2)^{1/2}\ UL/\alpha, \quad v = (Gr\ Pr^2)^{-1/4}\ VL/\alpha \\ t &= (T - T_\infty)/(T_w - T_\infty) \end{aligned}\right\} \tag{8}$$

If the limit of the momentum equation (7b) is taken as the Prandtl number vanishes, it becomes

$$uu_x + vu_y = t \tag{9}$$

which is equivalent to LeFevre's equation at the limit (ref. 7). This is a momentum equation for an inviscid fluid and, when taken with (7a) and (7c), provides heat-transfer rates that are approximately valid for fluids with very small Prandtl number. Of course, the condition of no slip at the boundary must be relaxed.

Viscous layer. - Reference to sketch (a) shows that, on the basis of the length scale used in the thermal region, the y-derivatives of the velocity components in the viscous layer become very large. Therefore, the viscous-layer thickness Δ_V at $X = L$ must be used for scaling rather than Δ_T. The dimensionless coordinate normal to the surface is designated

$$\overline{y} = Y/\Delta_V \tag{10a}$$

Such a change of scale for a coordinate affects the scaling of the corresponding velocity. Consequently,

$$V = \overline{V}^*\ \overline{v}(\overline{y}) \tag{10b}$$

The governing equations (1) become

$$u_x + \frac{\overline{V}^* L}{U^* \Delta_V} \overline{v}_{\overline{y}} = 0 \tag{11a}$$

$$uu_x + \frac{\overline{V}^* L}{U^* \Delta_V} \overline{v} u_{\overline{y}} = \frac{\nu L}{U^* \Delta_V^2} u_{\overline{yy}} + t \tag{11b}$$

$$ut_x + \frac{\overline{V}^* L}{U^* \Delta_V} \overline{v} t_{\overline{y}} = \frac{\alpha L}{U^* \Delta_V^2} t_{\overline{yy}} \tag{11c}$$

All the derivatives appearing in (11) are of unit order of magnitude in the viscous layer.

The continuity equation (11a) requires

$$\overline{V}^* = \frac{\Delta_V}{L} U^* \tag{12a}$$

In the viscous layer the viscous stress term is comparable in magnitude with the buoyancy force. Therefore,

$$\Delta_V = \sqrt{\frac{\nu L}{U^*}} \tag{12b}$$

The differential equations now take the form

$$u_x + \overline{v}_{\overline{y}} = 0 \tag{13a}$$

$$uu_x + \overline{v} u_{\overline{y}} = u_{\overline{yy}} + t \tag{13b}$$

$$\mathrm{Pr}(ut_x + \overline{v} t_{\overline{y}}) = t_{\overline{yy}} \tag{13c}$$

Here,

$$\overline{y} = (\mathrm{Gr})^{1/4} \, Y/L \tag{13d}$$

and

$$\overline{v} = (\mathrm{Gr})^{-1/4} \, VL/\nu \tag{13e}$$

The energy equation (13c) shows that for very small Prandtl number the temperature profile is nearly linear in the entire viscous region. This is a useful observation when applied to the construction of temperature profiles in the integral method.

Integral Method for Low Prandtl Number

Integrated equations of motion. - Either of the sets of differential equations (7) or (13) may be taken as the basis for an integral method. The selection of (7) emphasizes the thermal-layer thickness as the more fundamental of the two thicknesses because it is in the thermal layer that the buoyancy force acts to drive the flow. However, a slight change of view must be acknowledged in the transition from the differential equations to the integral equations. The thicknesses Δ_V and Δ_T at $X = L$ have so far been defined, in the discussion of the differential equations, only to order of magnitude because the solutions of the differential equations vanish only asymptotically as $Y \to \infty$. It is now necessary to make the definitions more precise and to let Δ_T represent the location of an interface between the thermal region of the boundary layer and the ambient fluid; at this boundary both the temperature difference and velocity vanish. The symbol Δ_T is retained for the thickness of the thermal region at $X = L$. At any other position X, the edge of this layer is given by

$$Y = \Delta_T \delta(x) \quad \text{or} \quad y = \delta(x) \tag{14a}$$

There is now also considered to be a sharp boundary between the viscous layer and the thermal layer, at which two kinds of profiles meet. A new parameter r is used to designate this boundary by writing at the edge of the viscous layer

$$Y = \Delta_T r\ \delta(x) \quad \text{or} \quad y = r\ \delta(x) \tag{14b}$$

At very small Prandtl number, by (5) and (12b),

$$r \approx \Delta_V/\Delta_T = \sqrt{Pr} \tag{15}$$

but, in general, r remains unspecified and must emerge from the solution of the problem. It should be noted that, with the use of only one boundary-layer-thickness variation $\delta(x)$, there is the tacit assumption that r is independent of x.

The momentum equation (7b) and the energy equation (7c) may be integrated from the wall to the outer edge of the thermal layer to yield

$$\frac{d}{dx}\int_0^\delta u^2\, dy = -\ Pr\ u_y(0) + \int_0^\delta t\, dy \tag{16a}$$

and

$$\frac{d}{dx}\int_0^\delta ut\, dy = -\ t_y(0) \tag{16b}$$

In deriving equations (16), the boundary conditions

$$v(0) = u(\delta) = t(\delta) = u_y(\delta) = t_y(\delta) = 0$$

have been used.

Temperature profiles. - Because the ratio of viscous to thermal layers varies with Prandtl number, it is convenient to represent the velocity and temperature profiles to be used in (16) by polynomials in each region, and to match them at the interface $y = r\,\delta(x)$. The polynomials in the viscous region are designated by a subscript 1 and those in the thermal region by a subscript 2.

The boundary conditions that the temperature profile must meet at the wall are

$y = 0$:

$$t_1 = 1, \quad t_{1,yy} = 0 \tag{17}$$

The second of these is obtained from the differential energy equation (7c). At the outer edge of the thermal layer the boundary conditions are

$y = \delta$:

$$t_2 = 0, \quad t_{2,y} = 0, \quad t_{2,yy} = 0 \tag{18}$$

The third condition arises from the energy equation again. The matching conditions on the polynomials are

$y = r\delta$:

$$t_1 = t_2, \quad t_{1,y} = t_{2,y} \tag{19}$$

As previously remarked, the energy equation (13c) shows that for small Prandtl number the profile may be well approximated by a linear function in the viscous layer. Hence, it is written (using eq. (17))

$$t_1 = 1 + a(y/\delta) \tag{20}$$

By equation (18) the profile in the thermal region must have a third-order zero at the outer edge. Thus,

$$t = b\left(1 - \frac{y}{\delta}\right)^3 \tag{21}$$

The constants a and b are determined by the matching conditions (eq. (19)), and the temperature profiles become

$$t_1 = 1 - \frac{3}{1 + 2r}\frac{y}{\delta} \tag{22a}$$

and

$$t_2 = \frac{1}{(1 - r)^2(1 + 2r)}\left(1 - \frac{y}{\delta}\right)^3 \tag{22b}$$

Velocity profiles. - The boundary conditions that the velocity profile must satisfy are

$y = 0$:

$$u_1 = 0, \qquad u_{1,yy} = -(Pr)^{-1}, \qquad u_{1,yyy} = -t_{1,y} \tag{23}$$

$y = \delta$:

$$u_2 = 0, \qquad u_{2,y} = 0 \tag{24a}$$

$y = r\delta$:

$$u_1 = u_2, \qquad u_{1,y} = u_{2,y} \tag{25}$$

The second of equations (23) comes from the momentum equation (7b). The third of equations (23) is obtained by differentiating the momentum equation with respect to y and using the condition of constant wall temperature, $t_x = 0$. This is a significant boundary condition because it relates the velocity profile directly to a quantity of primary interest, the heat transfer at the wall. Equation (7b), the momentum equation for the thermal layer, does not give unambiguous boundary conditions at low Pr on the higher derivatives of u at $y = \delta$. In appendix B it is shown by a study of the integral method at zero Prandtl number that a fourth-degree polynomial in the thermal region gives the best asymptotic results. Thus, two conditions are added to (24a):

$y = \delta$:

$$u_{2,yy} = u_{2,yyy} = 0 \tag{24b}$$

The lowest degree polynomials that satisfy all the conditions (eqs. (23) to (25)) are

$$u_1 = \frac{\delta^2(x)}{2Pr}\left[\frac{2r + 3r^2 + 3r^3}{(1 + 2r)(1 + 3r)}\frac{y}{\delta} - \left(\frac{y}{\delta}\right)^2 + \frac{1}{1 + 2r}\left(\frac{y}{\delta}\right)^3\right] \tag{26a}$$

$$u_2 = \frac{\delta^2(x)}{2Pr} \frac{r^2}{(1 - r)^3(1 + 2r)(1 + 3r)} \left(1 - \frac{y}{\delta}\right)^4 \tag{26b}$$

Solution of integrated equations. - Substitution of the temperature profiles (eqs. (22)) and the velocity profiles (eqs. (26)) into the integrals appearing in equations (16) yields

$$\int_0^\delta u^2 \, dy = \frac{\delta^5(x)}{3 \cdot 4 \cdot 5 \cdot 6 \cdot 7 Pr^2} \frac{r^4(70 + 126r + 189r^2 + 230r^3 + 99r^4 + 54r^5)}{(1 + 2r)^2(1 + 3r)^2} \tag{27a}$$

$$\int_0^\delta ut \, dy = \frac{\delta^3(x)}{15 \cdot 16 Pr} \frac{r^2(15 + 35r + 65r^2 + 53r^3 + 24r^4)}{(1 + 2r)^2(1 + 3r)} \tag{27b}$$

$$\int_0^\delta t \, dy = \frac{\delta(x)}{4} \frac{1 + 2r + 3r^2}{1 + 2r} \tag{27c}$$

Upon the introduction of the expressions (27) into the integrated equations, the latter become first-order differential equations for $\delta^4(x)$. The solutions are, for the momentum equation,

$$\delta^4(x) = \frac{Pr^2}{r^4} \frac{3 \cdot 4 \cdot 6 \cdot 7 \, (1 + r)(1 + 2r)(1 + 3r)(1 + 3r^2)x}{70 + 126r + 189r^2 + 230r^3 + 99r^4 + 54r^5} \tag{28a}$$

and, for the energy equation,

$$\delta^4(x) = \frac{Pr}{r^2} \frac{2^6 \cdot 3 \cdot 5 \, (1 + 2r)(1 + 3r)x}{15 + 35r + 65r^2 + 53r^3 + 24r^4} \tag{28b}$$

These two solutions for $\delta(x)$ must be identical; therefore their quotient can be used to obtain a relation between the parameters r and Pr.

$$Pr = \frac{40}{21} \frac{r^2(70 + 126r + 189r^2 + 230r^3 + 99r^4 + 54r^5)}{(1 + r)(1 + 3r^2)(15 + 35r + 65r^2 + 53r^3 + 24r^4)} \tag{29}$$

Equations (28a) - or (28b) - and (29) represent the solution of the low Prandtl number natural-convection flow. The customary result that the boundary layers grows like $x^{1/4}$ is clearly evident. Moreover, equation (29) yields, for small Pr, the value of the thickness ratio r that prescribes the profiles (22) and (26).

It is left now only to extract certain practical results. Before doing so, however, equation (29) is examined near its extreme values.

For $r << 1$,

$$r = \sqrt{9Pr/80} \tag{30}$$

a functional form already anticipated in equation (15). Figure 1 shows both the exact r - Pr relation, equation (29), and the asymptote, equation (30). The latter is seen to be adequate for $Pr < 0.01$. When the viscous layer is as large as the thermal layer, $r = 1$ and $Pr = 20/21$. This is the largest value of Prandtl number for which the method yields an answer.

Heat transfer and mass flow. - Figure 2 compares velocity profiles constructed from polynomials for $Pr = 0.003$, 0.03, and 0.72 with those found numerically by Sparrow and Gregg (ref. 8) and by Ostrach (ref. 4). The heavy dot marks the boundary between the viscous and thermal regions. The polynomials are more accurate for the two smaller Prandtl numbers then for $Pr = 0.72$. Having been tailored to the low Prandtl number extreme, they are not flexible enough to retain accuracy near $Pr = 1$. The same conclusions are drawn from a comparison of the corresponding temperature profiles (fig. 3). It is also apparent that the temperature profiles quickly approach an asymptotic form below $Pr \approx 10^{-2}$.

The heat transfer may be described nondimensionally at any position on the plate by the local Nusselt number

$$Nu \equiv -\frac{X}{T_w - T_\infty}\left(\frac{\partial T}{\partial Y}\right)_w = -(Gr_X Pr^2)^{1/4}\,\frac{x^{1/4}}{\delta}\left(\frac{\partial t}{\partial (y/\delta)}\right)_w \tag{31}$$

Customarily the average Nusselt number $\overline{Nu} = (4/3)Nu$ is used as the measure of gross heat transfer. The quantity

$$\overline{Nu}(Gr_X Pr^2)^{-1/4} = -\frac{4}{3}\,\frac{x^{1/4}}{\delta}\left(\frac{\partial t}{\partial (y/\delta)}\right)_w = \frac{4}{1 + 2r}\,\frac{x^{1/4}}{\delta} \tag{32}$$

is nearly independent of Pr and may be evaluated by using equations (22a), (28), and (29). It is plotted in figure 4 for $0.0001 \leq Pr \leq 1$. For comparison the same quantity is shown as given by the interpolation formula of LeFevre (ref. 7), which is based on numerical calculations, and by the methods of Squire and Fujii. It is seen that the results of the latter methods diverge from the numerical solution as Pr becomes vanishingly small, but the present integral method becomes very accurate. In fact, asymptotically equation (32) becomes

$$\overline{Nu}(Gr_X Pr^2)^{-1/4} = 0.8190 \tag{33}$$

which compares favorably with LeFevre's asymptotic formula,

$$\overline{Nu}(Gr_X Pr^2)^{-1/4} = 0.8005 \tag{34}$$

These asymptotic formulas are adequate for $Pr \leq 0.01$.

Another significant test of the integral method is the prediction of mass flow in the boundary layer. The mass flow for a plate of width L is

$$M = L\rho \int_0^\infty U \, dY \tag{35}$$

or, nondimensionally,

$$\frac{M}{\rho \alpha L} (Gr_X Pr^2)^{-1/4} = \frac{\delta^3}{x^{3/4}} \int_0^1 \frac{u}{\delta^2} \, d\left(\frac{y}{\delta}\right) \tag{36}$$

The right side of equation (36) may be evaluated from equations (26), (28), and (29) and is a slowly varying function of Pr. Equation (36) is plotted in figure 5 for $0.0001 \leq Pr \leq 1$. For comparison, the numerical computations of references 4 and 8 and the results of Squire's and Fujii's methods are shown. The present method is the most accurate integral method in the important liquid-metal range of Prandtl numbers, $Pr \leq 0.05$. As $Pr \to 0$, equation (36) becomes

$$\frac{M}{\rho \alpha L} (Gr_X Pr^2)^{-1/4} = 1.310 \tag{37}$$

FLAT-PLATE FLOW AT HIGH PRANDTL NUMBER

Differential Equations at High Prandtl Number

In fluids that have a large Prandtl number the viscous effects penetrate much farther into the fluid than the thermal effects. This is illustrated in sketch (b), in which Δ_T and Δ_V represent, respectively, distances from the wall which the temperature and velocity profiles at $X = L$ drop to at least an order of magnitude below their maximum values. All of the impulse is transmitted to the fluid in the thermal layer, and the fluid beyond $Y = \Delta_T$ is dragged along by the viscous forces. Again, as with the boundary layer at low Prandtl number, the qualitative aspects of the flow can best be examined by nondimensionalizing the differential equations.

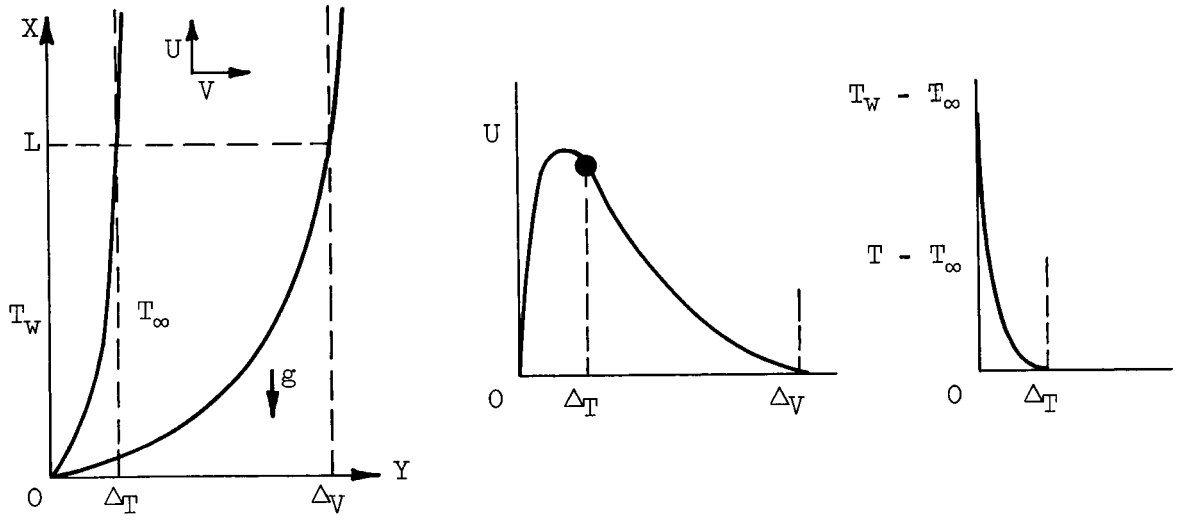

(b)

Thermal region. - Consider the dimensional equations of motion (1) again to be transformed by equations (2) to yield the dimensionless equations (3). Three physical conditions are imposed to determine the characteristic quantities U^*, V^*, Δ_T. In the continuity equation (3a), it is again required that the terms be of the same order of magnitude:

$$V^*L/U^*\Delta_T = 1 \tag{38a}$$

Because the fluid is very viscous, in the thermal region the viscous force is comparable with the buoyancy force. In the momentum equation (3b), this leads to

$$\nu L/U^*\Delta_T^2 = g\beta(T_w - T_\infty)L/U^{*2} \tag{38b}$$

Finally, in the energy equation (3c), the conduction and convection of heat must balance:

$$\alpha L/U^*\Delta_T^2 = 1 \tag{38c}$$

From equations (38) there result

$$V^* = U^*\Delta_T/L \tag{39a}$$

$$U^* = \sqrt{\frac{g\beta(T_w - T_\infty)L}{Pr}} \tag{39b}$$

$$\Delta_T/L = (Gr\ Pr)^{-1/4} \equiv (Ra)^{-1/4} \tag{39c}$$

Two significant differences from the low Prandtl number case are observed in equations (39). First, the characteristic velocity depends on the Prandtl number, falling to zero for large values of that parameter; and, second, the coordinate scaling now involves the Rayleigh number alone. Although the form (39b) for U^* has not appeared explicitly in the literature, it is equivalent to nondimensionalizations made previously for large Prandtl number (e.g., refs. 9 to 11).

It is now possible to write the equations of motion in the form appropriate to the thermal layer:

$$u_x + v_y = 0 \tag{40a}$$

$$(uu_x + vu_y)/Pr = u_{yy} + t \tag{40b}$$

$$ut_x + vt_y = t_{yy} \tag{40c}$$

where

$$\left.\begin{aligned} x = X/L, \qquad y = Ra^{1/4}\, Y/L, \qquad u = Ra^{-1/2}\, UL/\alpha \\ v = Ra^{-1/4}\, VL/\alpha, \qquad t = (T - T_\infty)/(T_w - T_\infty) \end{aligned}\right\} \tag{41}$$

The momentum equation (40b) exhibits very clearly the condition that the viscous and buoyancy forces be of the same order of magnitude. In fact, for $Pr \to \infty$ the inertia terms drop out, and the equation becomes

$$u_{yy} + t = 0 \tag{42}$$

which is equivalent to LeFevre's limiting equation (ref. 7). The boundary conditions associated with equation (42) are

$Y = 0$:

$$u = 0 \tag{43a}$$

$Y = \Delta_T$:

$$u_y = \Delta_T\, u_Y = \frac{\Delta_T}{\Delta_V} \frac{\partial u}{\partial (Y/\Delta_V)} \to 0 \tag{43b}$$

The second of these makes use of the fact that $\Delta_T/\Delta_V \to 0$ as $Pr \to \infty$, while $\partial u/\partial(Y/\Delta_V)$ is of order unity at the juncture of the two layers.

Viscous layer. - In the viscous layer (sketch (b)) there are no thermal effects, but the major portion of the mass flow occurs there. The governing equations in the dimensionless form (11), along with the

conditions that both terms of the continuity equation must be retained and that the inertia and viscous forces balance while the buoyancy is negligible, yield

$$u_x + \overline{v}_{\overline{y}} = 0 \tag{44a}$$

$$uu_x + \overline{v}u_{\overline{y}} = u_{\overline{yy}} \tag{44b}$$

where

$$\overline{y} = Y/\Delta_V, \qquad \Delta_V = \overline{V}^* L/U^*$$

The characteristic velocity U^* for these equations is that for the thermal region, equation (39b). The velocity must match that at the edge of the thermal layer and vanish at the edge of the viscous layer.

Integral Method for High Prandtl Number

Integrated equations. - The construction of the integral method for large Prandtl number follows the general scheme employed for low Prandtl number, modified according to the change in governing equations, and allowing for the inversion in relative size of the thermal and viscous layers. Again, the loose descriptions of the layer thicknesses used in discussing the differential equations are replaced by sharp definitions. At the edge of the thermal layer the temperature difference now vanishes exactly, and at the edge of the viscous layer the velocity profile vanishes exactly.

The edge of the thermal layer is defined by

$$Y = \Delta_T\, \delta(x) \qquad \text{or} \qquad y = \delta(x) \tag{45a}$$

and the edge of the viscous layer by

$$Y = \Delta_T \delta(x)/R \qquad \text{or} \qquad y = \delta(x)/R \tag{45b}$$

where, for very large Prandtl number,

$$R \approx \Delta_T/\Delta_V = 1/\sqrt{Pr} \tag{45c}$$

In terms of these definitions, the integration of the differential equations (40) yields

$$(1/Pr)\, \frac{d}{dx} \int_0^{\delta/R} u^2\, dy = -u_y(0) + \int_0^{\delta/R} t\, dy \tag{46a}$$

and

$$\frac{d}{dx}\int_0^{\delta/R} ut\, dy = -t_y(0) \tag{46b}$$

The foregoing equations are to be solved for the boundary-layer thickness $\delta(x)$ and the parameter R. As before, the profiles representing u and t in equation (46) are constructed separately in the two regions. It is this division of the problem that assures the successful prediction of heat- and mass-transfer trends by the integral method, and not the details of the construction in each region. To illustrate this point, the solution of the problem with a temperature profile satisfying seven boundary conditions is compared with the solution obtained when the profile satisfies four boundary conditions. Both sets of profiles yield acceptable results.

Sixth-degree temperature profile. - The boundary conditions satisfied by this temperature profile at the wall are

$y = 0$:

$$t_1 = 1, \qquad t_{yy} = 0, \qquad t_{1,yyy} = 0 \tag{47a}$$

The second of these is the energy equation evaluated at the wall, and the third comes from the derivative of the energy equation with the condition of constant wall temperature imposed. At the edge of the thermal layer the conditions imposed are

$y = \delta$:

$$t_1 = t_{1,y} = t_{1,yy} = t_{1,yyy} = 0 \tag{47b}$$

The conditions for the second and third derivatives again arise from the energy equation. The last boundary condition has not been used in the low Prandtl number case. The polynomial that meets the conditions (47) is

$$t_1 = 1 - 2(y/\delta) + 5(y/\delta)^4 - 6(y/\delta)^5 + 2(y/\delta)^6 \tag{48}$$

The boundary conditions on the velocity polynomials u_1 in the thermal layer and u_2 in the viscous layer are

$y = 0$:

$$u_1 = 0 \tag{49a}$$

$y = \delta$:

$$u_1 = u_2, \qquad u_{1,y} = u_{2,y} \tag{49b}$$

$y = \delta/R$:

$$u_2 = u_{2,y} = 0 \tag{49c}$$

To insure proper behavior of the velocity polynomial at infinite Prandtl number, the limiting form of the momentum equation

$$u_{1,yy} = -t_1 \tag{42}$$

is integrated in the thermal region to relate the polynomial to the temperature profile. There results, using boundary conditions (49a,b),

$$u_1 = \frac{1}{84}\left[4\left(\frac{6 + 13R}{1 + 3R}\right)\frac{y}{\delta} - 42\left(\frac{y}{\delta}\right)^2 + 28\left(\frac{y}{\delta}\right)^3 - 14\left(\frac{y}{\delta}\right)^6 + 12\left(\frac{y}{\delta}\right)^7 - 3\left(\frac{y}{\delta}\right)^8\right]\delta^2(x) \tag{50a}$$

A study of the results of Stewartson and Jones (ref. 12), who repeated LeFevre's computation of the thermal layer at infinite Prandtl number and, in addition, computed the velocity profile in the viscous layer, shows that the velocity profile in the viscous region can be well represented by a fourth-degree term. Application of the boundary conditions (49b,c) yields

$$u_2 = \frac{5}{84}\,\frac{1}{(1 + 3R)(1 - R)^3}\,[1 - R(y/\delta)]^4\,\delta^2(x) \tag{50b}$$

The integrals that arise in the equations of motion (46) are

$$\int_0^{\delta/R} u^2\,dy = \frac{55,250 + 211,623R + 533,808R^2 + 304,567R^3}{2^5 \cdot 3^4 \cdot 5 \cdot 7^2 \cdot 13 \cdot 17R(1 + 3R)^2}\,\delta^5(x) \tag{51a}$$

$$\int_0^{\delta} ut\,dy = \frac{12,294 + 19,007R}{2^2 \cdot 3^2 \cdot 5 \cdot 7^2 \cdot 11 \cdot 13(1 + 3R)}\,\delta^3(x) \tag{51b}$$

$$\int_0^{\delta} t\,dy = \frac{2}{7}\,\delta(x) \tag{51c}$$

Introduction of these quantities into the momentum and energy equation (46) yields two first-order differential equations for $\delta(x)$ that have the solutions

Momentum:

$$\delta^4(x) = \frac{\mathrm{Pr}\, R^2\, 2^7 \cdot 3^3 \cdot 5 \cdot 7 \cdot 13 \cdot 17\ (1 + 3R)}{55,250 + 211,623R + 533,808R^2 + 304,567R^3}\, x \qquad (52a)$$

Energy:

$$\delta^4(x) = \frac{2^5 \cdot 3 \cdot 5 \cdot 7^2 \cdot 11 \cdot 13(1 + 3R)}{12,294 + 19,007R}\, x \qquad (52b)$$

The ratio of the equivalent solutions (52a) and (52b) yields the Pr - R relation,

$$\mathrm{Pr} = \frac{7 \cdot 11}{2^2 \cdot 3^2 \cdot 17}\, \frac{55,250 + 211,623R + 533,808R^2 + 304,567R^3}{R^2(12,294 + 19,007R)} \qquad (53)$$

When the thermal layer becomes as thick as the viscous layer,

$$R = 1, \qquad \mathrm{Pr} = 4.44 \qquad (54)$$

This is the lowest value of Pr at which the method yields an answer. At very high Prandtl numbers,

$$R = \sqrt{0.5654/\mathrm{Pr}} \qquad (55)$$

a relation of the form (45c).

Figure 6 shows the R - Pr relation and figures 7 and 8 show velocity and temperature profiles at Pr = 10, 100, 1000. In figure 7 comparisons with numerical solutions (ref. 4) reveal that, while the velocity polynomials are accurate in the forepart of the thermal region ($y/\delta < 0.5$), they depart from the true profiles in the viscous region, especially at the lower Prandtl number. The temperature profile (fig. 8) is a very close approximation to the real profiles, which are nearly identical for the three Prandtl numbers.

The qualities of the profiles show up also in the integrated parameters, mean Nusselt number, and mass flow. From the definition of Nusselt number, equation (31), it follows that for high Prandtl number flows the mean Nusselt number is

$$\overline{\mathrm{Nu}} = -\frac{4}{3}\, (\mathrm{Ra}_x)^{1/4}\, \frac{x^{1/4}}{\delta} \left(\frac{\partial t}{\partial (y/\delta)} \right)_w \qquad (56)$$

This relation is plotted in figure 9 for values of Prandtl number greater than 4.44. Comparison with LeFevre's interpolation formula shows that the integral method is a suitable representation of the heat transfer over its applicable range. This is also evident from the asymptotic form of (56),

$$\overline{Nu}\ Ra_x^{-1/4} = (5.410)^{-1/4} = 0.6557 \tag{57}$$

LeFevre has a slightly greater numerical factor:

$$\overline{Nu}\ Ra_x^{-1/4} = (4.95)^{-1/4} = 0.6704 \tag{58}$$

The asymptotic form should be adequate above $Pr = 1000$.

The Nusselt number as given by Squire's method and by Fujii's method is also shown. All three integral methods have the correct qualitative behavior. Squire's method is the most accurate at very high Prandtl numbers.

The mass flow as defined by equation (35) is described nondimensionally at large Prandtl number by

$$\frac{M\ Ra_x}{\rho(\nu\alpha)^{1/2}\ L} = \frac{\delta^3}{x^{3/4}} \frac{42 + 91R + 147R^2}{2^3 \cdot 3^2 \cdot 7^2 (1 + 3R)(R^2 Pr)^{1/2}} \tag{59}$$

This relation is compared in figure 10 with numerical computations and the other integral methods. The latter, although yielding good values in the lower range of Prandtl number, depend on the Prandtl number in an improper fashion and, therefore, indicate the wrong order of magnitude at large values of the parameter. Asymptotically at $Pr = \infty$, equation (59) becomes

$$\frac{M\ Ra_x^{-1/4}}{\rho(\nu\alpha)^{1/2} L} = 1.065 \tag{60}$$

The number in (60) is somewhat lower than the number 1.216 obtained from the solution of Stewartson and Jones (ref. 12) and shown in figure 10.

Third-degree temperature profile. - Only four boundary conditions will be imposed on the temperature profile.

$y = 0$:

$$t = 1, \qquad t_{yy} = 0$$

$y = \delta$: (61)

$$t = t_y = 0$$

Therefore,

$$t_1 = 1 - \frac{3}{2}\frac{y}{\delta} + \frac{1}{2}\left(\frac{y}{\delta}\right)^3 \tag{62}$$

The velocity polynomials are determined by equation (42) and the boundary conditions equations (49) to be

$$u_1 = \frac{1}{40}\left[\frac{15 + 7R}{1 + R}\frac{y}{\delta} - 20\left(\frac{y}{\delta}\right)^2 + 10\left(\frac{y}{\delta}\right)^3 - \left(\frac{y}{\delta}\right)^5\right]\delta^2(x) \tag{63a}$$

and

$$u_2 = \frac{1}{10}\frac{1}{(1 + R)(1 - R)}\left(1 - R\frac{y}{\delta}\right)^2 \delta^2(x) \tag{63b}$$

Integrals appearing in the integrated equations of motion are

$$\int_0^{\delta/R} u^2\, dy = \frac{11088 + 5551R + 7934R^2 - 1313R^3}{2^6 \cdot 3^2 \cdot 5^3 \cdot 7 \cdot 11 \cdot R(1 + R)^2}\,\delta^5(x) \tag{64a}$$

$$\int_0^{\delta} ut\, dy = \frac{275 + 23R}{2^3 \cdot 3^2 \cdot 5^2 \cdot 7(1 + R)}\,\delta^3(x) \tag{64b}$$

$$\int_0^{\delta} t\, dy - u_y(0) = \frac{R}{5(1 + R)}\,\delta(x) \tag{64c}$$

Solutions to the integrated equations are

Momentum:

$$\delta^4(x) = 2^8 \cdot 3^2 \cdot 5 \cdot 7 \cdot 11(Pr)\,\frac{R^2(1 + R)}{11088 + 5551R + 7934R^2 - 1313R^3}\,x \tag{65a}$$

Energy:

$$\delta^4(x) = 2^4 \cdot 3^2 \cdot 5^2 \cdot 7\,\frac{1 + R}{275 + 23R}\,x \tag{65b}$$

and the Pr - R relation is

$$Pr = \frac{5}{2^4 \cdot 11}\,\frac{11088 + 5551R + 7934R^2 - 1313R^3}{R^2(275 + 23R)} \tag{66}$$

Asymptotically for large Pr, equation (66) becomes

$$R = \sqrt{1.145/Pr} \tag{67}$$

The minimum Pr for which the method can yield a solution is determined, by setting R = 1 in equation (66), to be

$$Pr = 2.217 \tag{68}$$

This value is less than the corresponding minimum value found for the previous method (4.44). The R - Pr relation (66) and the corresponding lower limit (68) are shown in figure 6.

Figures 11 and 12 compare the velocity and temperature profiles at Pr = 10, 100, 1000 with numerical solutions of reference 4. The velocity polynomials are not as close to the true profiles in the viscous region as could be desired, but both they and the temperature polynomials are near to the exact solutions in the thermal region. The heat transfer and mass flow are shown in figures 9 and 10, respectively. The asymptotic forms of the heat-transfer and mass-flow parameters are

$$\overline{Nu}\ Ra_x^{-1/4} = 0.646 \tag{69}$$

and

$$\frac{M\ Ra_x^{-1/4}}{\rho(\nu\alpha)^{1/2}\ L} = 0.922 \tag{70}$$

Thus, both the heat-transfer and mass-flow predictions are lower than those made by the higher degree polynomials (eqs. (57) and (60)) and the numerical computations. Graphical comparisons are made in figures 9 and 10.

APPLICATION TO CONE

Small Prandtl Number

The integral methods that have been developed can be applied to flows over other bodies than the flat plate, provided the flow has the property of similarity. As an illustration, consider the flow over a cone at small Prandtl number.

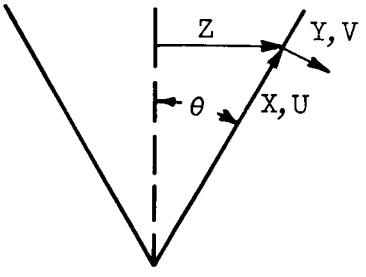

(c)

The surface of the cone is given by

$$Z = X \sin \theta \tag{71}$$

and, if the boundary layer is "thin", (71) also describes Z for it. The differential equations are (ref. 13):

$$\frac{\partial}{\partial X}(ZU) + \frac{\partial}{\partial Y}(ZV) = 0 \tag{72a}$$

$$U\frac{\partial U}{\partial X} + V\frac{\partial U}{\partial Y} = \nu\frac{\partial^2 U}{\partial Y^2} + \sqrt{1 - \left(\frac{dZ}{dX}\right)^2}\,\beta g(T - T_\infty) \tag{72b}$$

$$U\frac{\partial T}{\partial X} + V\frac{\partial T}{\partial Y} = \alpha\frac{\partial^2 T}{\partial Y^2} \tag{72c}$$

After multiplication by Z and application of the transformations (10) and (13) - with Gr based on $g \cos \theta$, the equations may be integrated to yield

$$\frac{1}{x}\frac{d}{dx}\,x\int_0^\delta u^2\,dy = -\,Pr\left(\frac{\partial u}{\partial y}\right)_w + \int_0^\delta t\,dy \tag{73a}$$

$$\frac{1}{x}\frac{d}{dx}\,x\int_0^\delta ut\,dy = -\left(\frac{\partial t}{\partial y}\right)_w \tag{73b}$$

Assuming that the u and t profiles on the cone and flat plate are not too different, integrals occurring in equation (73) are those already used in the flat-plate problem (eqs. (27)). From the solutions of these equations there results for the r - Pr relation,

$$Pr = \frac{27}{35}(Pr)_{fp} \tag{74}$$

where $(Pr)_{fp}$ is the functional dependence of Pr on r given for the flat plate in equation (29).

The mean heat transfer can also be related to that for the flat plate. Using again the definition (31) for the Nusselt number, the Nusselt number based on the mean temperature gradient at the wall is given by

$$\overline{Nu}(Gr_x Pr^2)^{-1/4} = 2\left(\frac{5}{49}\right)^{1/4}\left[\overline{Nu}(Gr_x Pr^2)^{-1/4}\right]_{fp} \tag{75}$$

In this formula the Prandtl numbers for the cone and flat plate are related by (74), and Gr_x for the cone is based on $g \cos \theta$. From (33) the asymptotic form of (75) is obtained as $Pr \to 0$:

$$\overline{Nu}(Gr_x Pr^2)^{-1/4} = 0.926 \tag{76}$$

Heat Transfer on Cone at Infinite Prandtl Number

The integral methods described here are especially rapid if only the asymptotic form of the flow is needed. The solution of the flow over a cone at infinite Prandtl number illustrates this point. The differential equations (72) are transformed according to (41) and, after multiplication by Z, integrate to

$$0 = -\left(\frac{\partial u}{\partial y}\right)_w + \int_0^\delta t \, dy \tag{77}$$

$$\frac{1}{x}\frac{d}{dx} x \int_0^\delta ut \, dy = -\left(\frac{\partial t}{\partial y}\right)_w \tag{78}$$

Equation (77) is automatically satisfied because its differential form is used to relate the temperature and velocity profiles (eq. (42)). The solution of (78) is (using eqs. (51b) and (48))

$$\delta^4 = \frac{2^4 \cdot 5 \cdot 7 \cdot 11 \cdot 13}{683} x \tag{79}$$

From equations (48) and (79) the mean temperature gradient at the wall is

$$\left(\overline{\frac{\partial t}{\partial y}}\right)_w = -\frac{16}{7}\left(\frac{683}{2^4 \cdot 5 \cdot 7 \cdot 11 \cdot 13x}\right)^{1/4} = \frac{8}{7}\left(\frac{\partial t}{\partial y}\right)_w \tag{80}$$

The Nusselt number based on the temperature gradient (80) is given by

$$\overline{Nu}\ Ra_x^{-1/4} = 0.695 \tag{81}$$

where Ra_x is based on $g \cos \theta$.

In the computations outlined here for $Pr = \infty$, the complicated R - Pr relation does not occur. For this reason the derivation of the heat-transfer relation (81) is much simplified. The number appearing in equation (81) is about 25 percent higher than the value 0.555 given by Merk and Prins (ref. 10), who employed the method of Squire.

CONCLUDING REMARKS

By concentrating on an analysis of the differential equations at very high and very low Prandtl number, integral methods that are of value over a wide range of that parameter have been developed. The principal value of the two methods, however, is probably the ease with which heat transfer and mass flow can be found for the limiting cases of infinite and zero Prandtl number. The main quantity of interest in natural-convection flows is the heat transfer. This has been found fairly accurately for a flat plate because the temperature profiles closely reproduce the known real solutions. In general, the method should yield reasonably good solutions also to natural-convection flows in the liquid-metal and viscous-oil ranges on other bodies.

Some interesting observations can be made about the similarity properties of the flows studied herein. First, it is apparent that in the thermal region there is a similarity among the profiles, in the low Prandtl number range and also in the high. This is certainly to be expected, because it is in the thermal region that the driving force for the flow operates. The scaling parameters that emerge are Gr Pr (Rayleigh number) for large Pr flows and Gr Pr^2 for small Pr. The latter parameter is entirely independent of viscosity, which is only natural, since viscosity has little effect on low Prandtl number flows. It should be noted that, although it is customary to say that there is no characteristic velocity in natural-convection flows as there is in forced convection, this means only that there is no velocity imposed by boundary conditions on the velocity field. Actually, characteristic velocities do arise from the balance of forces in the motion, as shown herein for both extremes of Prandtl number.

Lewis Research Center
National Aeronautics and Space Administration
Cleveland, Ohio, April 14, 1960

APPENDIX A

SYMBOLS

a,b	constants
Gr	Grashof number, $\frac{\beta g(T_w - T_\infty)L^3}{\nu^2}$
Gr_X	Grashof number based on X, $\frac{\beta g(T_w - T_\infty)X^3}{\nu^2}$
g	acceleration of gravity
L	characteristic length of body
M	mass flow
Nu	Nusselt number, $\frac{-X}{T_w - T_\infty}\left(\frac{\partial T}{\partial Y}\right)_w$
$\overline{Nu}$	Nusselt number based on mean temperature gradient at wall
Pr	Prandtl number, ν/α
p,q	constants
R	ratio of thermal- to viscous-layer thickness at large Pr
Ra	Rayleigh number, Pr Gr
Ra_X	Rayleigh number based on X, Pr Gr_X
r	ratio of viscous- to thermal-layer thickness at small Pr
T	temperature
t	dimensionless temperature difference, $(T - T_\infty)/(T_w - T_\infty)$
U,V	velocity components (sketches (a) to (c))
u,v	dimensionless velocity components
X,Y,Z	coordinates (sketches (a) to (c))

x,y	dimensionless coordinates
α	thermal diffusivity
β	coefficient of thermal expansion
Δ	dimensional layer thickness at distance L from leading edge
$\delta(x)$	dimensionless layer thickness at position x along plate or cone
θ	cone angle
ν	kinematic viscosity
ρ	mass density

Subscripts:

fp	flat plate
T	thermal layer
V	viscous layer
w	wall value
X,Y,x,y	partial derivatives
∞	value in ambient fluid
1	smaller of thermal and viscous layers
2	larger of thermal and viscous layers

Superscripts:

*	characteristic value
$\bar{}$	bar over letter designates variable in viscous layer (except $\overline{Nu}$)

APPENDIX B

CHOICE OF u_2 AT LOW PRANDTL NUMBER

To choose the best form of the velocity profile in the thermal region at low Prandtl number, proceed to the extreme case of $Pr = 0$. In this case the profiles need be specified only in the thermal region. Let the velocity profile have a zero of degree p at the outer edge of the thermal layer, and the temperature profile a zero of degree q. The variation in the numerical constant in the asymptotic heat transfer formula, equation (33), is shown in the left-hand table.

q	p		
	2	3	4
2	0.7848	0.7792	0.7677
3	.8165	.8223	.8192
4	.8255	.8400	.8433

q	p		
	2	3	4
2	1.15	1.36	1.55
3	1.00	1.18	1.34
4	.892	1.06	1.20

Comparison of the values in the table with the LeFevre's value, 0.8005, shows that q should be in the range $2 < q < 3$. The choice of p is not apparent.

Another test of the effect of profile index is obtained by integrating the momentum equation (7b) at the wall for $Pr = 0$. At $x = 1$, it is found that $u = \sqrt{2}$. The approximations which the various polynomial combinations make to this number are shown in the right-hand table. Only a choice of $p = 4$ can lead to a sufficiently large value of u at the wall. Thus, both the indices p and q have been chosen.

REFERENCES

1. Eckert, E. R. G.: Introduction to the Transfer of Heat and Mass. McGraw-Hill Book Co., Inc., 1950.

2. Goldstein, S., ed.: Modern Developments in Fluid Dynamics. Vol. II. Clarendon Press (Oxford), 1938.

3. Levy, Salomon: Integral Methods in Natural-Convection Flow. Jour. Appl. Mech., vol. 22, no. 4, Dec. 1955, pp. 515-522.

4. Ostrach, Simon: An Analysis of Laminar Free-Convection Flow and Heat Transfer About a Flat Plate Parallel to the Direction of the Generating Body Force. NACA Rep. 1111, 1953. (Supersedes NACA TN 2635.)

5. Yamagata, Kiyoshi: An Analysis of Free-Convection About a Vertical Plate. Trans. Japan Soc. Mech. Eng., vol. 24, no. 144, Aug. 1958, pp. 541-546. (English summary.)

6. Fujii, Tetsu: Some Considerations on the Mathematical Analysis of Heat-Transfer from a Vertical Flat Surface by Laminar Free-Convection. Trans. Japan Soc. Mech. Eng., vol. 24, no. 148, Dec. 1958, pp. 957-963. (English summary.)

7. LeFevre, E. J.: Laminar Free Convection from a Vertical Plane Surface. Heat Div. Paper 113, Dept. Sci. and Ind. Res., Mech. Eng. Lab., Aug. 1956.

8. Sparrow, E. M., and Gregg, J. L.: Details of Exact Low Prandtl Number Boundary-Layer Solutions for Forced and for Free Convection. NASA MEMO 2-27-59E, 1959.

9. Saunders, O. A.: Natural Convection in Liquids. Proc. Roy. Soc. (London), ser. A, vol. 172, no. 948, July 19, 1939, pp. 55-71.

10. Merk, H. J., and Prins, J. A.: Thermal Convection in Laminar Boundary Layers. Appl. Sci. Res., sec. A, pt. I, vol. 4, no. 1, 1953, pp. 11-24; pt. II, vol. 4, no. 3, 1954, pp. 195-228.

11. Morgan, George W., and Warner, W. H.: On Heat Transfer in Laminar Boundary Layers at High Prandtl Number. Jour. Aero. Sci., vol. 23, no. 10, Oct. 1956, pp. 937-948.

12. Stewartson, K., and Jones, L. T.: The Heated Vertical Plate at High Prandtl Number. Jour. Aero. Sci., vol. 24, no. 5, May 1957, pp. 379-380.

13. Goldstein, S., ed.: Modern Developments in Fluid Dynamics. Vol. I. Clarendon Press (Oxford), 1938.

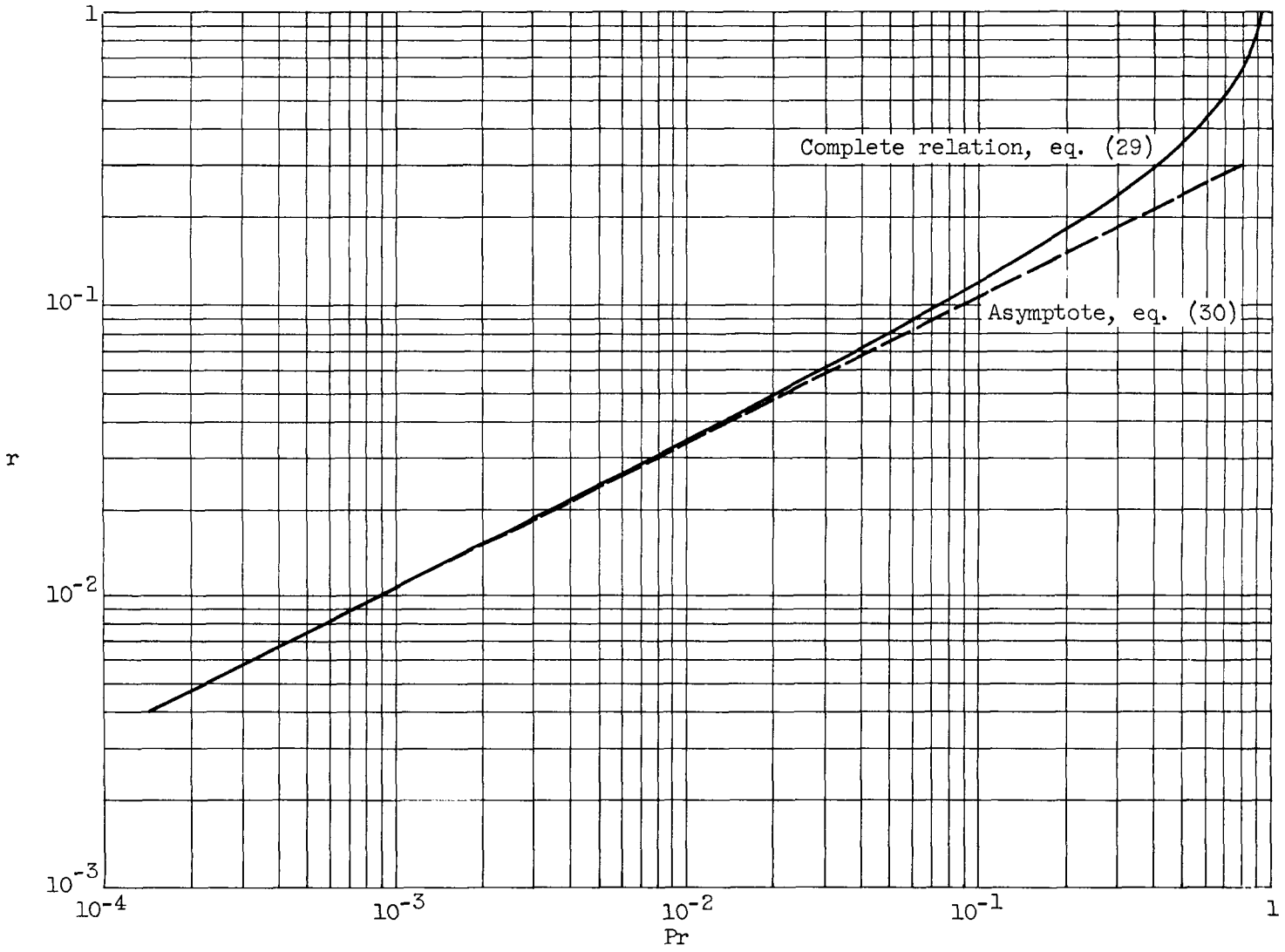

Figure 1. - Layer thickness ratio at low Prandtl number.

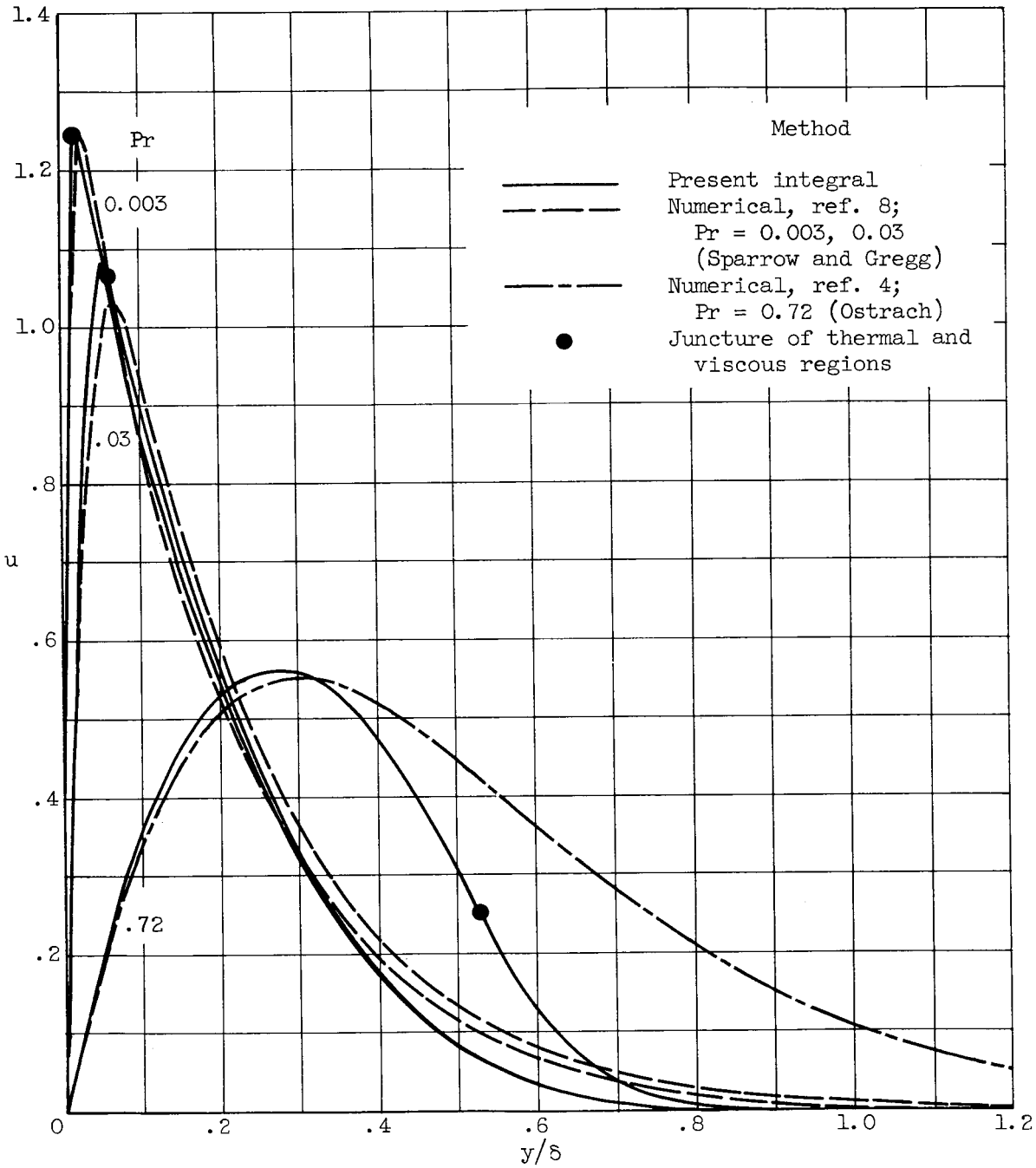

Figure 2. - Velocity profiles, low Prandtl number.

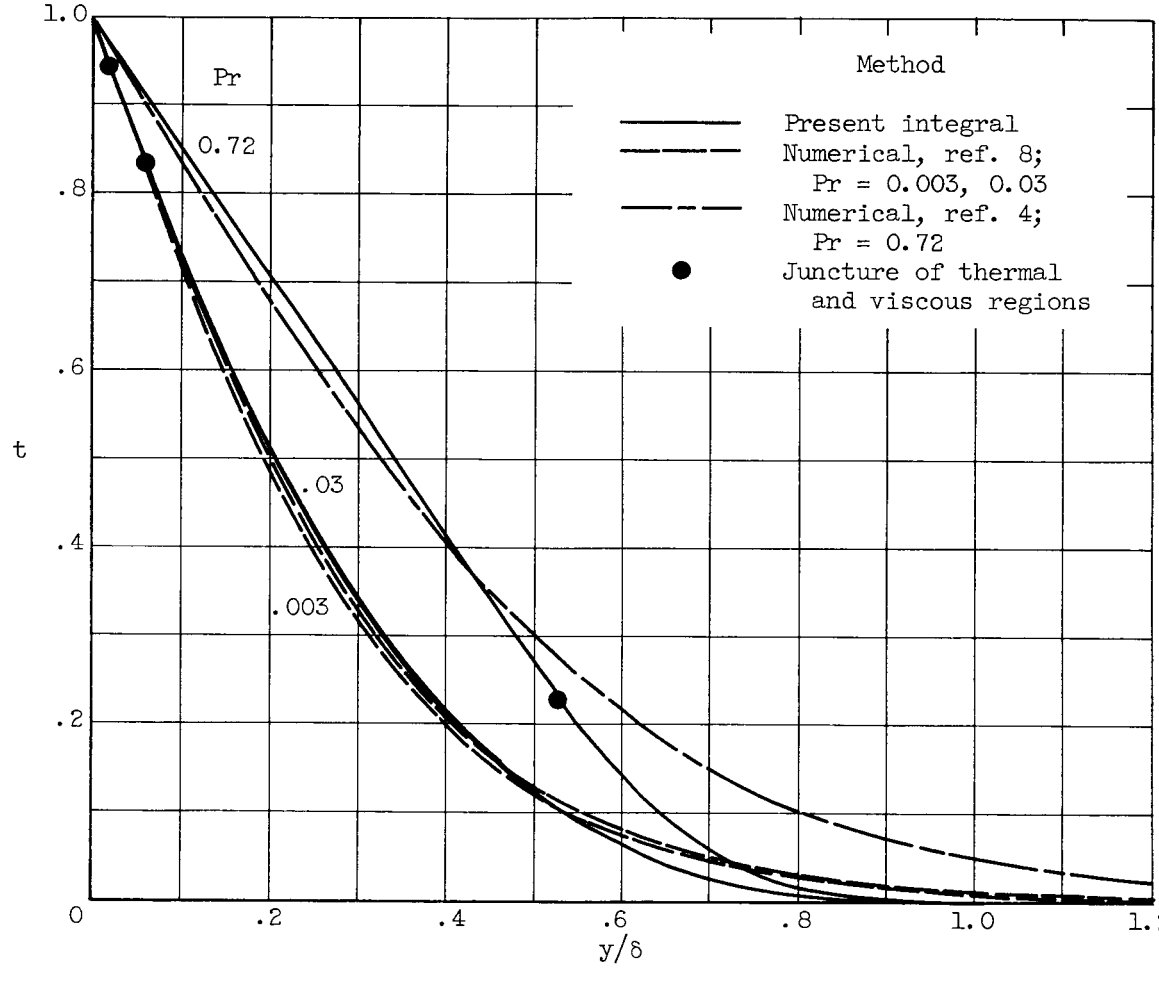

Figure 3. - Temperature profiles, low Prandtl number.

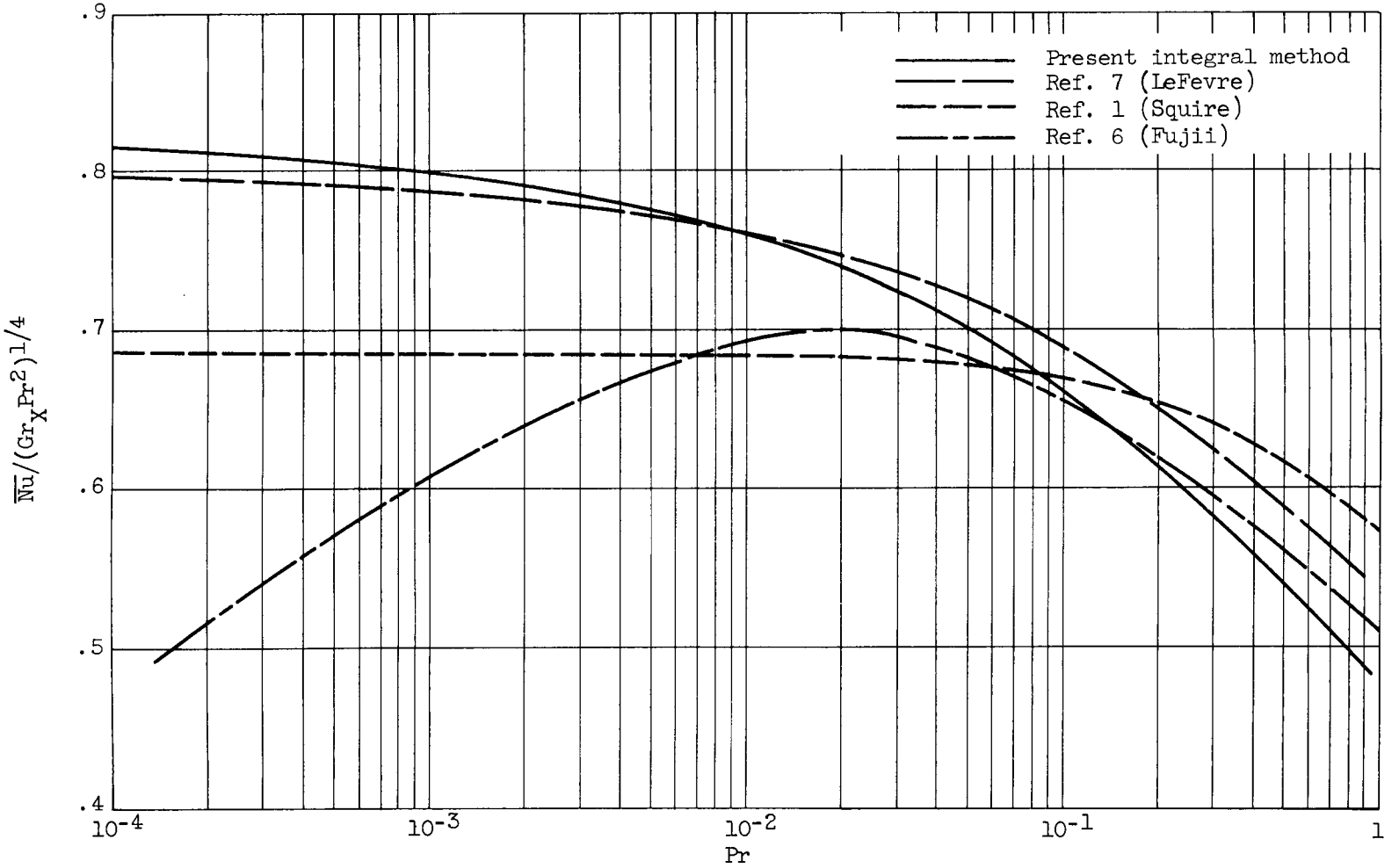

Figure 4. - Heat transfer from a flat plate, low Prandtl number.

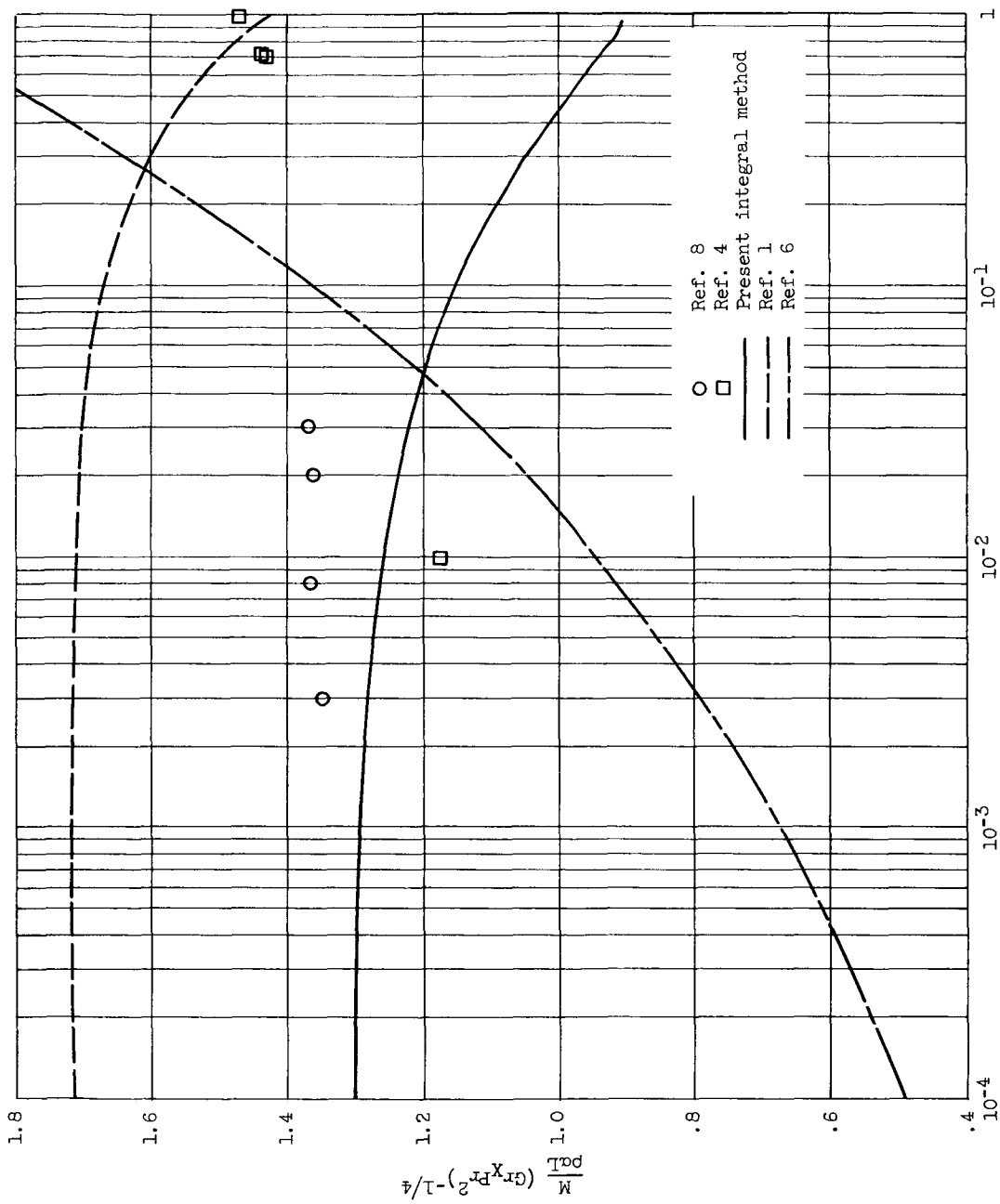

Figure 5. - Mass flow on a flat plate, low Prandtl number.

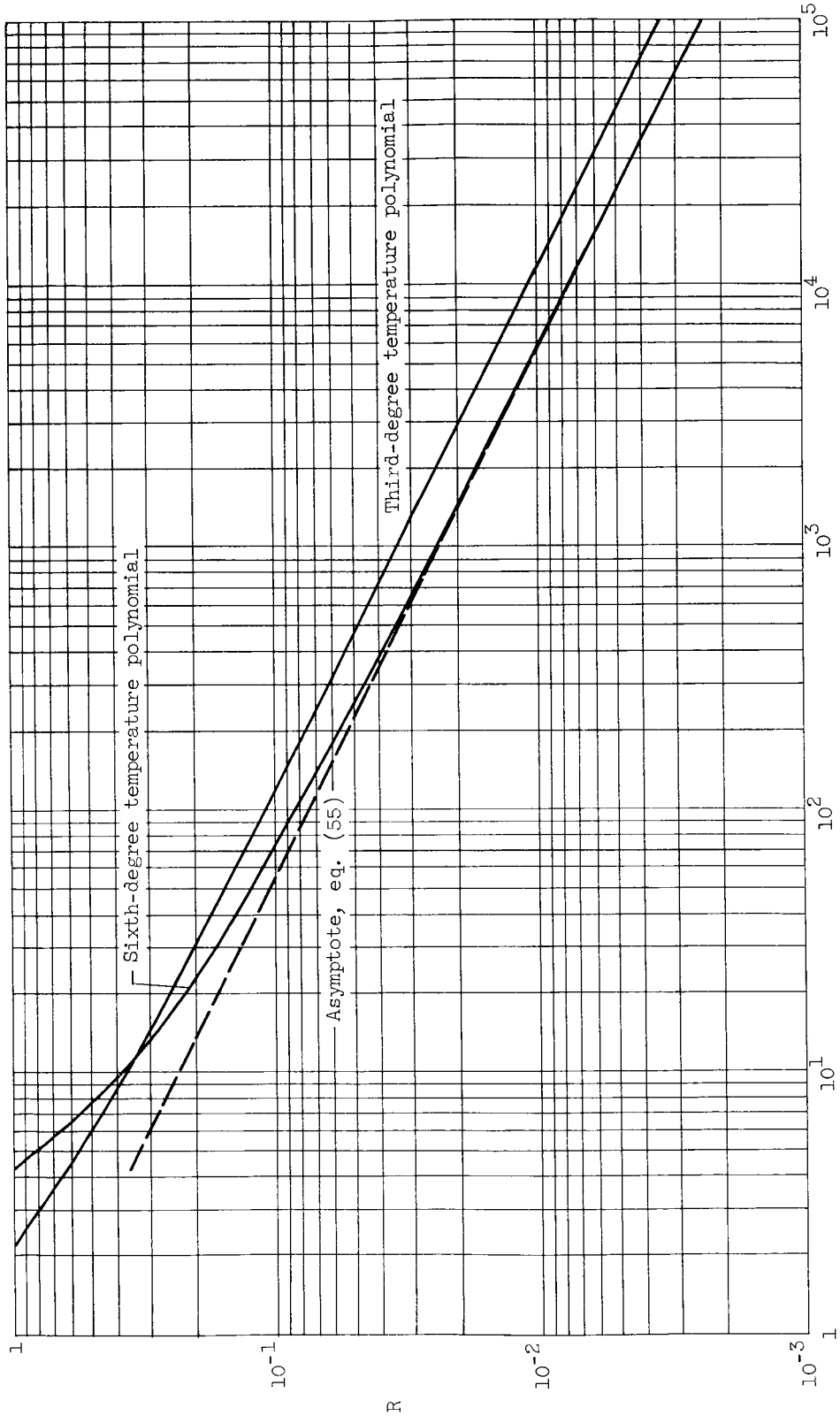

Figure 6. - Layer thickness ratio at high Prandtl number.

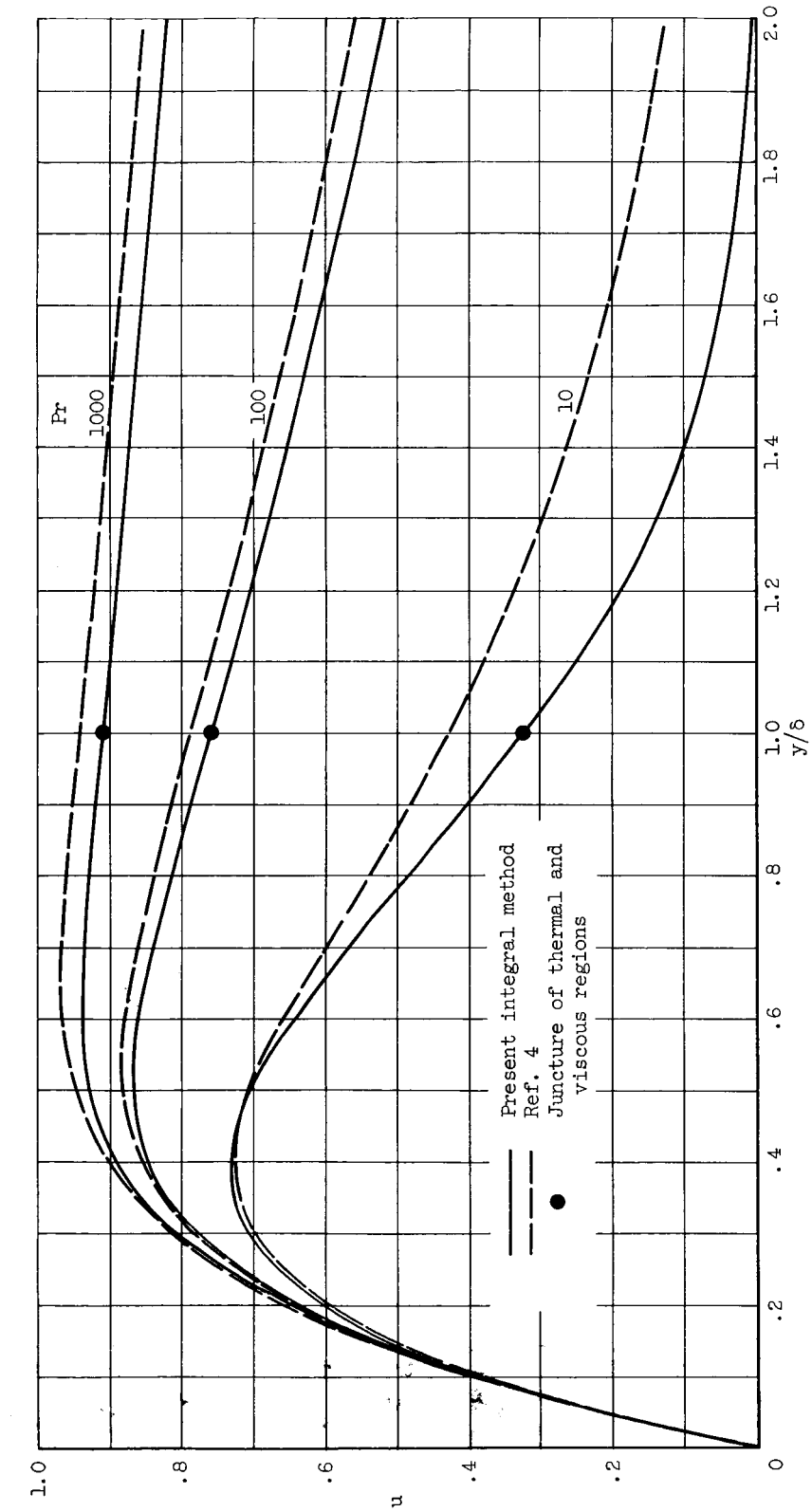

Figure 7. - Velocity profiles at high Prandtl number. Sixth-degree associated temperature polynomial.

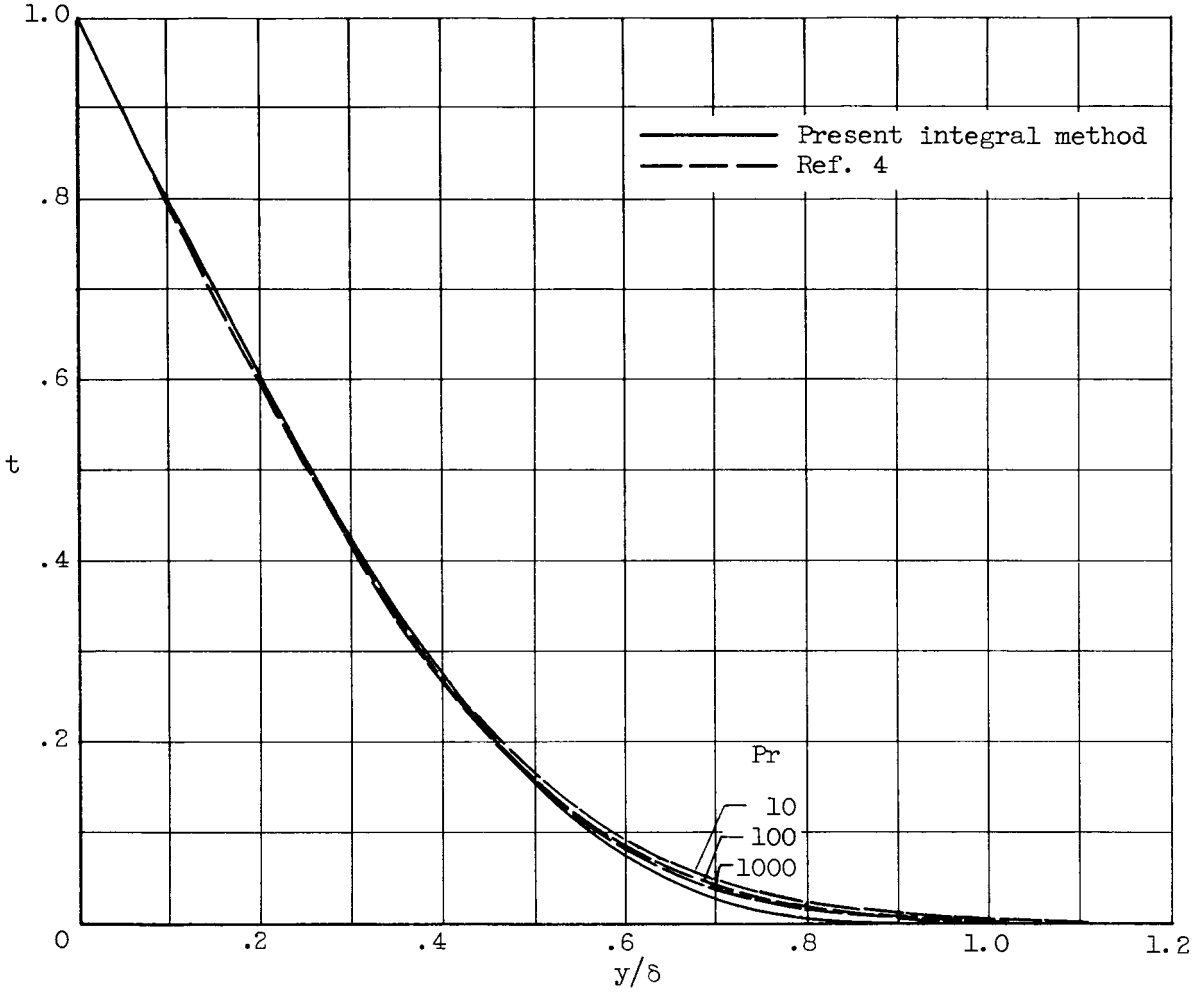

Figure 8. - Temperature profiles at high Prandtl number.

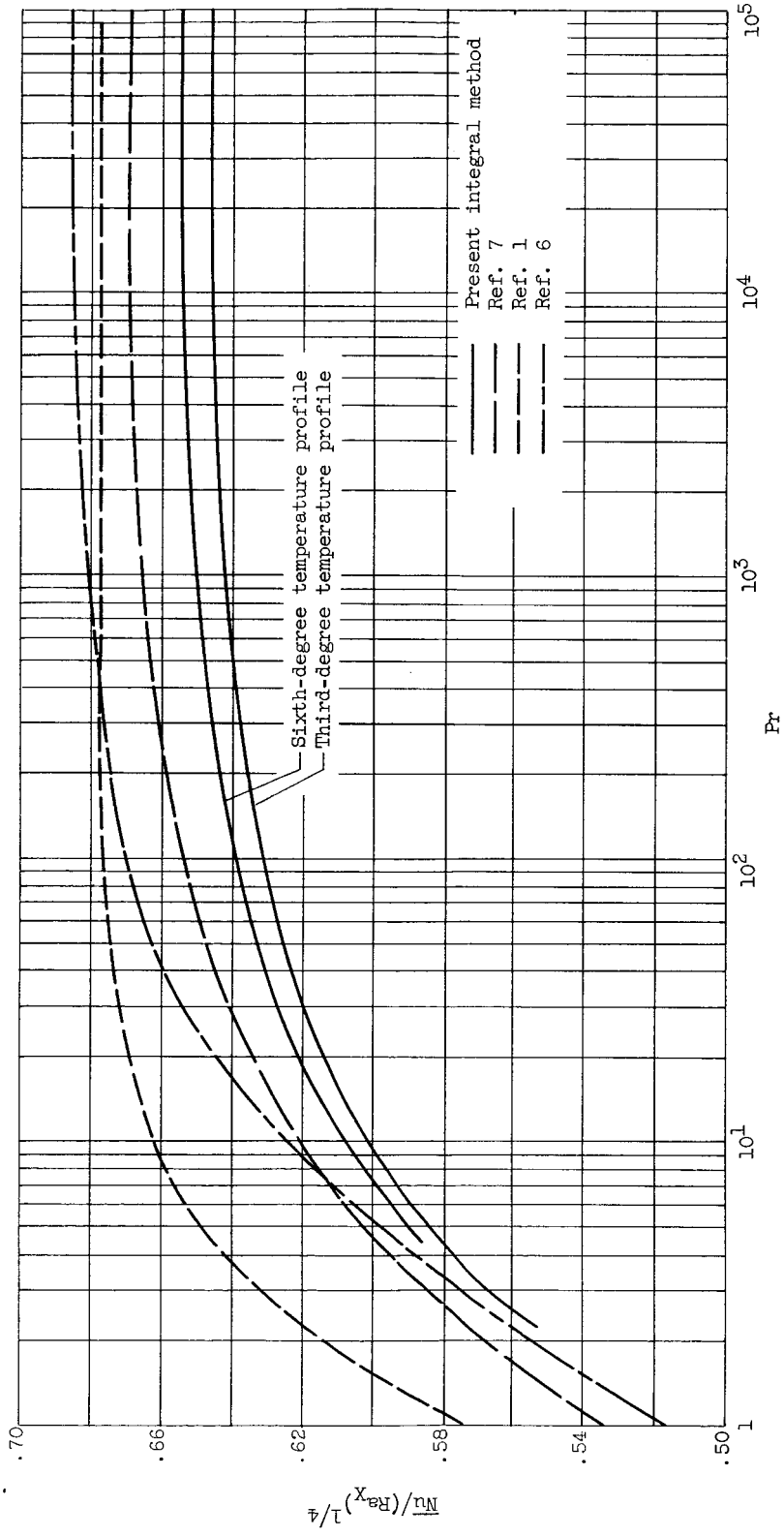

Figure 9. - Heat transfer from a flat plate, high Prandtl number.

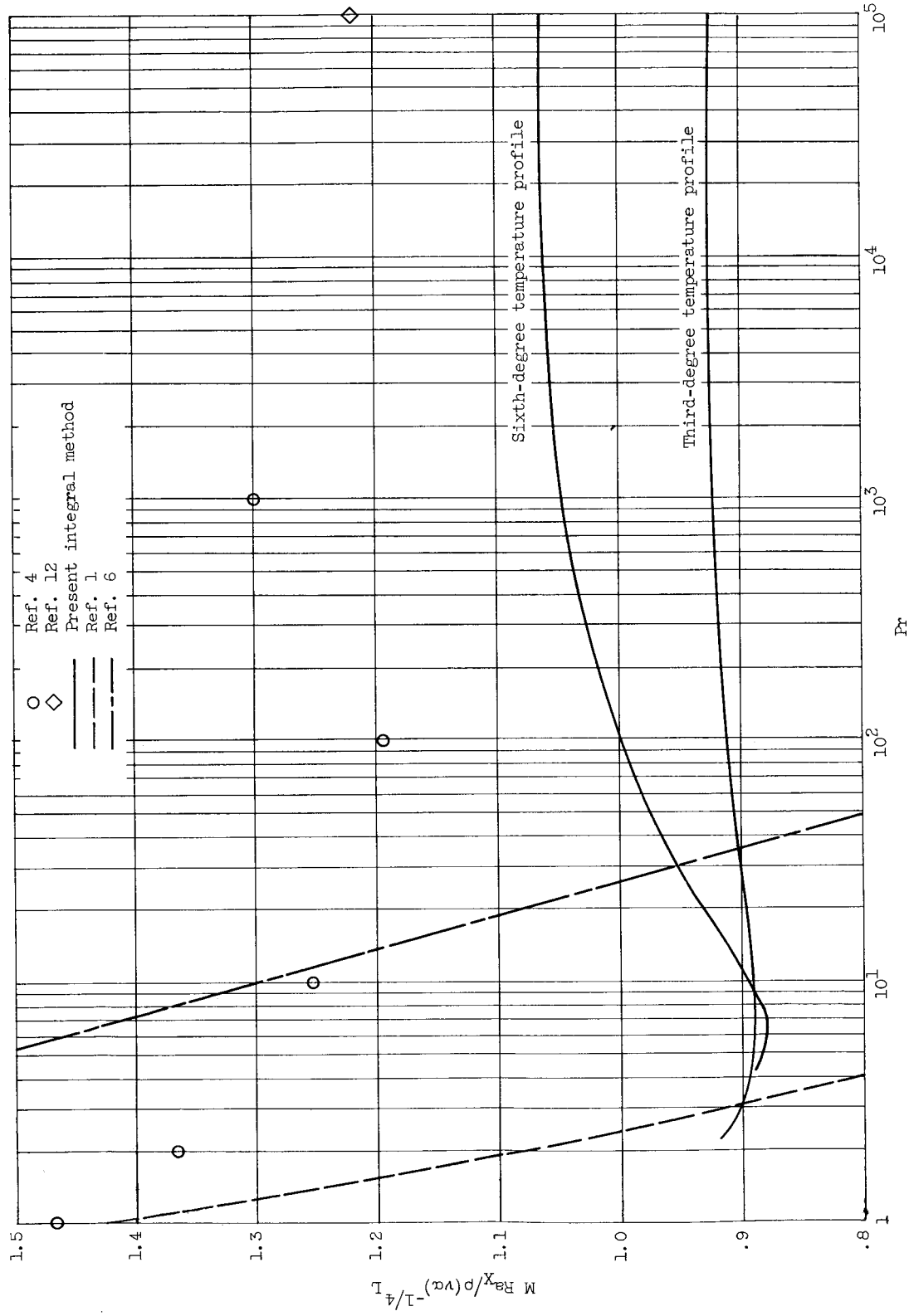

Figure 10. - Mass flow over a flat plate, high Prandtl number.

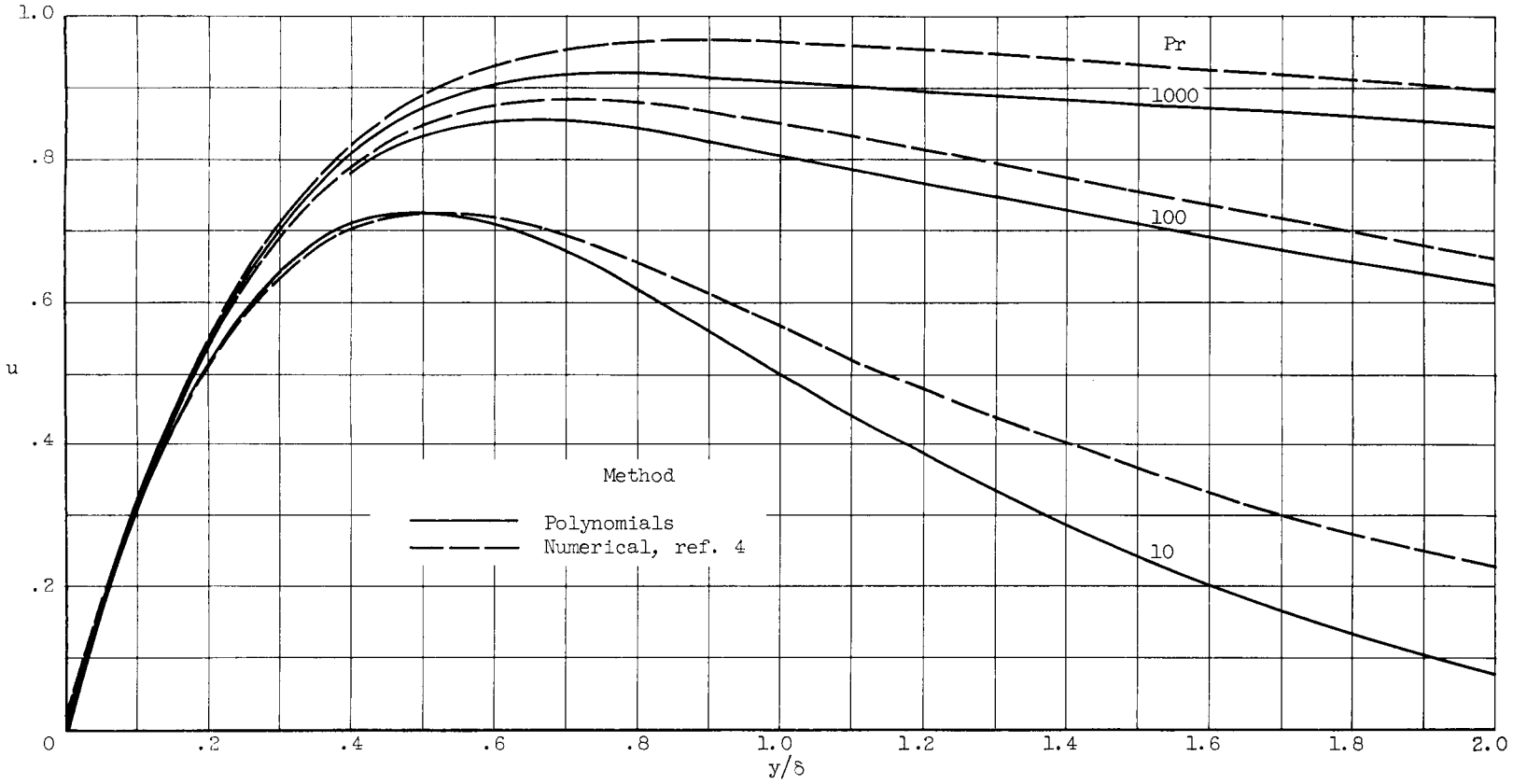

Figure 11. - Velocity profiles at high Prandtl number. Third-degree associated temperature profiles.

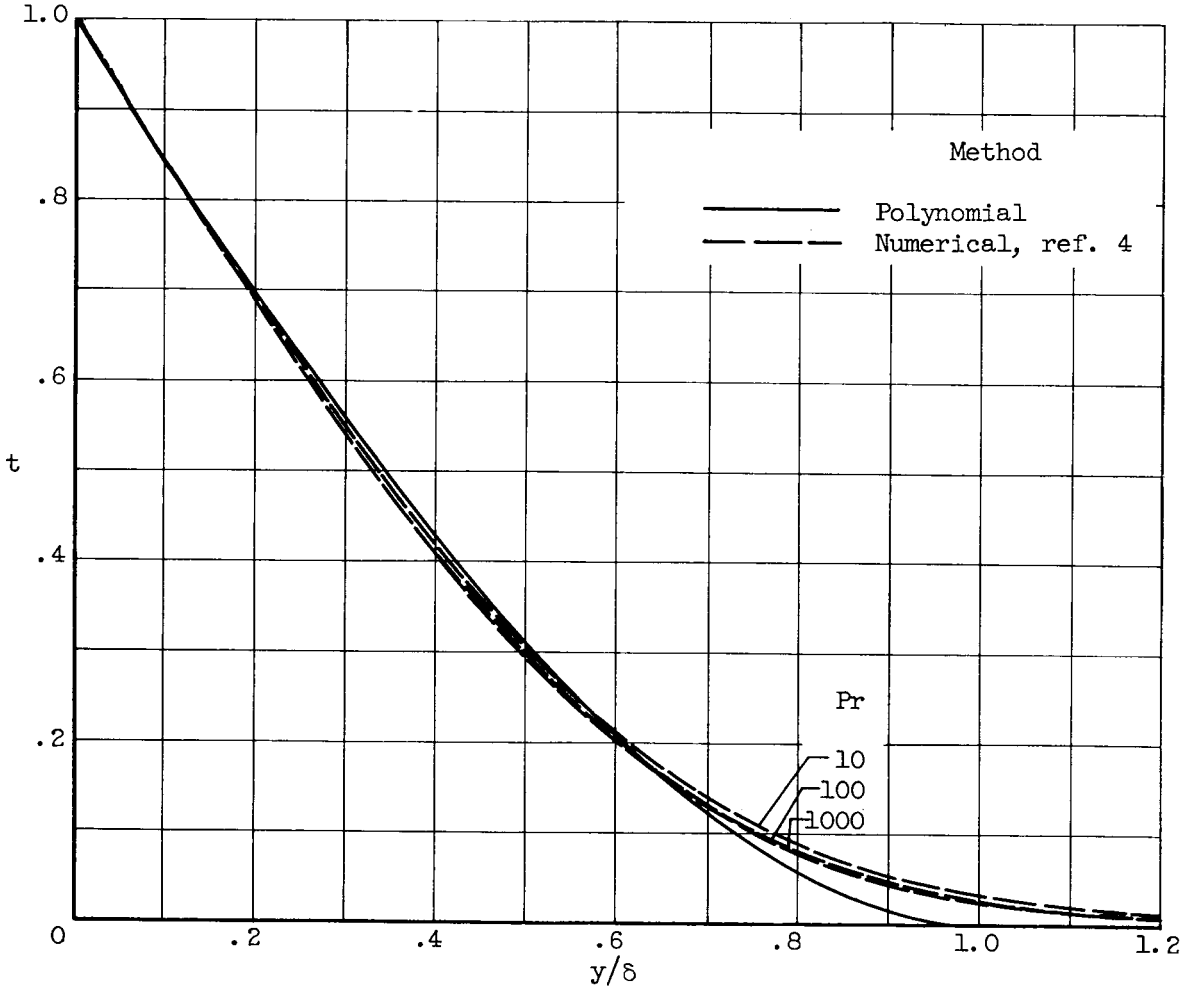

Figure 12. - Third-degree temperature profile, high Prandtl number.